DELPHI Collaboration

DELPHI 2002-04 CONF 545
February 18, 2002

Preliminary S-Matrix Fits to LEP 1 and LEP 2 DELPHI Data

G.Della Ricca[1], J.Holt[2], A.Olchevski[3]

Abstract

The hadronic and leptonic cross-sections and leptonic forward-backward asymmetries determined from the data collected with the DELPHI detector at energies near the Z^0 resonance peak (88-93 GeV) and above (130-209 GeV) during LEP operations between 1990 and 2000 have been interpreted in terms of the S-matrix parameters.

[1]INFN, Trieste, Italy
[2]CERN, Geneva, Switzerland
[3]Joint Institute for Nuclear Research, Dubna, Russia

1 Introduction

The published measurements of [1], [2], [3] and the preliminary results of [4] and [5] were analyzed in the framework of the S-matrix approach, achieving a substantial improvement in the precision of the γZ^0 interference compared to the accuracy obtained from the Z^0 data alone [1], updating the results presented in [2].

2 Interpretation of the results in the S-matrix formalism

The S-matrix formalism is a rigorous model independent approach to describe the cross-sections and the forward-backward asymmetries in the e^+e^- annihilations. In this model, the cross-sections can be parametrized as follows:

$$\sigma_a^0(s) = \frac{4}{3}\pi\alpha^2 \left[\frac{\mathrm{g_f}^a}{s} + \frac{\mathrm{j_f}^a (s - \overline{\mathrm{M}}_\mathrm{Z}^2) + \mathrm{r_f}^a\, s}{(s - \overline{\mathrm{M}}_\mathrm{Z}^2)^2 + \overline{\mathrm{M}}_\mathrm{Z}^2 \overline{\Gamma}_\mathrm{Z}^2} \right] \quad \text{with} \quad \begin{array}{l} a = \mathrm{tot, fb} \\ \mathrm{f} = \mathrm{had, e}, \mu, \tau \,, \end{array} \tag{1}$$

while the forward-backward asymmetries are given by:

$$A_{\mathrm{fb}}^0(s) = \frac{3}{4} \frac{\sigma_{\mathrm{fb}}^0(s)}{\sigma_{\mathrm{tot}}^0(s)} \,, \tag{2}$$

where $\sqrt{s}$ is the centre-of-mass energy. The parameters $\mathrm{r_f}$ and $\mathrm{j_f}$ scale the Z^0 exchange and the γZ^0 interference contributions to the total cross-section and forward-backward asymmetries. The contribution $\mathrm{g_f}$ of the pure γ exchange was fixed to the value predicted by QED in all fits. The Z^0 exchange term, the γZ^0 interference term and the photon exchange term are given by:

$$\begin{aligned}
\mathrm{r_f^{tot}} &= \kappa^2 \left[\hat{a}_e^2 + \hat{v}_e^2 \right] \left[\hat{a}_f^2 + \hat{v}_f^2 \right] - 2\kappa\, \hat{v}_e\, \hat{v}_f C_{Im} \\
\mathrm{j_f^{tot}} &= 2\kappa\, \hat{v}_e\, \hat{v}_f\, (C_{Re} + C_{Im}) \\
\mathrm{g_f^{tot}} &= Q_\mathrm{e}^2 Q_\mathrm{f}^2 \, |F_A(\mathrm{M_Z})|^2 \\
\mathrm{r_f^{fb}} &= 4\kappa^2 \hat{a}_e\, \hat{v}_e\, \hat{a}_f\, \hat{v}_f - 2\kappa\, \hat{a}_e\, \hat{a}_f C_{Im} \\
\mathrm{j_f^{fb}} &= 2\kappa\, \hat{a}_e\, \hat{a}_f\, (C_{Re} + C_{Im}) \\
\mathrm{g_f^{fb}} &= 0 \,,
\end{aligned} \tag{3}$$

with the following definitions:

$$\begin{aligned}
\kappa &= \frac{G_F \mathrm{M_Z}^2}{2\sqrt{2}\,\pi\alpha} \approx 1.50 \\
C_{Im} &= \frac{\Gamma_\mathrm{Z}}{\mathrm{M_Z}}\, Q_\mathrm{e} Q_\mathrm{f}\, \mathrm{Im}\left\{ F_A(\mathrm{M_Z}) \right\} \\
C_{Re} &= Q_\mathrm{e} Q_\mathrm{f}\, \mathrm{Re}\left\{ F_A(\mathrm{M_Z}) \right\} \\
F_A(\mathrm{M_Z}) &= \frac{\alpha(\mathrm{M_Z})}{\alpha} \,,
\end{aligned} \tag{4}$$

where $\alpha(M_Z)$ is the complex fine-structure constant, and $\alpha \equiv \alpha(0)$. The photonic virtual and bremsstrahlung corrections are included through the convolution of Equation 1 with the photonic flux function.

Fits to the measured inclusive and non-radiative hadronic and leptonic cross-sections and leptonic forward-backward asymmetries were carried out in this framework using the corresponding branch of the ZFITTER/SMATASY6.36 [6, 7, 8] program [1]. The fits included hadronic and leptonic DELPHI measurements performed near the Z^0 resonance [1], and hadronic, muon and tau measurements at higher energies [2, 3, 4, 5].

The usual definitions of the mass M_Z and width Γ_Z of a Breit-Wigner resonance were used, the width being s-dependent:

$$\begin{aligned} M_Z &\equiv \overline{M}_Z\sqrt{1+\overline{\Gamma}_Z{}^2/\overline{M}_Z{}^2} \approx \overline{M}_Z + 34.20 \text{ MeV}/c^2 \\ \Gamma_Z &\equiv \overline{\Gamma}_Z\sqrt{1+\overline{\Gamma}_Z{}^2/\overline{M}_Z{}^2} \approx \overline{\Gamma}_Z + 0.94 \text{ MeV}. \end{aligned} \quad (5)$$

The results of the fits are presented in Table 1. The χ^2 amounted to 162.2(236.9) in the case of the 16-parameter fit (i.e. without assuming lepton universality) and to 176.5(246.5) for the 8-parameter fit (where lepton universality was assumed), for the line-shape and the combined line-shape and high energy data, respectively, the number of fitted points being 177(237). The correlation coefficients between the free parameters of the 16- and 8-parameter fits for the LEP1 and LEP1+LEP2 are shown in Tables 2, 3, 4 and 5. The data support the hypothesis of lepton universality. Overall, the measurements are in good agreement with the Standard Model predictions.

The correlations between the parameters M_Z and j^{tot}_{had} is shown in Figure 1. It can be seen that a significant improvement on the precision on the hadronic interference parameter, j^{tot}_{had}, is obtained when the high energy data are included in the fit.

[1]The following values for the Standard Model parameters were used: $M_Z = 91.1875$ GeV, $m_t = 175$ GeV, $M_H = 150$ GeV, $\alpha_s = 0.118$, $\Delta\alpha^{(5)}_{had} = 2.8761 \times 10^{-2}$ and $G_F = 1.166389 \times 10^{-5}$ GeV^{-2}. The following ZFITTER flags were used: AFBC: 1 SCAL: 0 SCRE: 0 AMT4: 4 BORN: 0 BOXD: 1 CONV: 1 FINR: 1 FOT2: 3 GAMS: 1 DIAG: 1 INTF: 1 BARB: 2 PART: 0 POWR: 1 PRNT: 0 ALEM: 2 QCDC: 3 VPOL: 1 WEAK: 1 FTJR: 1 EXPR: 0 EXPF: 0 HIGS: 0 AFMT: 1 CZAK: 0 PREC:10 HIG2: 0 ALE2: 3 GFER: 2 ISPP: 2 FSRS: 1 MISC: 0 MISD: 1 IPFC: 5 IPSC: 0 IPTO: 3 FBHO: 0 FSPP: 0 FUNA: 0 ASCR: 1 SFSR: 1 ENUE: 1 TUPV: 1 .

	LEP1		LEP1+LEP2		SM
M_Z	91.1939 ± 0.0112	91.1826 ± 0.0094	91.1857 ± 0.0037	91.1841 ± 0.0036	–
Γ_Z	2.4861 ± 0.0048	2.4886 ± 0.0046	2.4890 ± 0.0041	2.4889 ± 0.0041	2.497
r_{had}^{tot}	2.9490 ± 0.0110	2.9544 ± 0.0106	2.9557 ± 0.0096	2.9554 ± 0.0096	2.966
r_e^{tot}	0.14092 ± 0.00095		0.14125 ± 0.00091		
r_μ^{tot}	0.14274 ± 0.00072		0.14295 ± 0.00067		
r_τ^{tot}	0.14161 ± 0.00100		0.14201 ± 0.00096		
r_ℓ^{tot}		0.14230 ± 0.00062		0.14235 ± 0.00058	0.1427
j_{had}^{tot}	-0.21 ± 0.64	0.54 ± 0.54	0.36 ± 0.14	0.39 ± 0.14	0.22
j_e^{tot}	-0.095 ± 0.074		-0.050 ± 0.047		
j_μ^{tot}	0.056 ± 0.042		0.022 ± 0.020		
j_τ^{tot}	0.040 ± 0.046		-0.007 ± 0.026		
j_ℓ^{tot}		0.047 ± 0.037		0.006 ± 0.016	0.004
r_e^{fb}	0.00306 ± 0.00092		0.00298 ± 0.00091		
r_μ^{fb}	0.00275 ± 0.00051		0.00286 ± 0.00049		
r_τ^{fb}	0.00416 ± 0.00072		0.00428 ± 0.00070		
r_ℓ^{fb}		0.00304 ± 0.00038		0.00326 ± 0.00037	0.00273
j_e^{fb}	0.803 ± 0.073		0.805 ± 0.073		
j_μ^{fb}	0.711 ± 0.037		0.797 ± 0.024		
j_τ^{fb}	0.707 ± 0.047		0.822 ± 0.032		
j_ℓ^{fb}		0.726 ± 0.027		0.804 ± 0.019	0.799

Table 1: Results of the 16- and 8-parameter fits to the line-shape and combined line-shape and high energy data. Also shown are the Standard Model predictions for the fit parameters.

	Γ_Z	r^{tot}_{had}	r^{tot}_{e}	r^{tot}_{μ}	r^{tot}_{τ}	j^{tot}_{had}	j^{tot}_{e}	j^{tot}_{μ}	j^{tot}_{τ}	r^{fb}_{e}	r^{fb}_{μ}	r^{fb}_{τ}	j^{fb}_{e}	j^{fb}_{μ}	j^{fb}_{τ}
M_Z	-0.50	-0.46	-0.29	-0.32	-0.25	-0.96	-0.81	-0.70	-0.64	0.13	0.25	0.16	-0.03	0.00	0.00
Γ_Z		0.90	0.52	0.67	0.49	0.53	0.41	0.38	0.35	-0.06	-0.11	-0.07	0.04	0.04	0.03
r^{tot}_{had}			0.53	0.68	0.49	0.50	0.38	0.36	0.32	-0.05	-0.10	-0.06	0.04	0.05	0.04
r^{tot}_{e}				0.39	0.28	0.30	0.26	0.22	0.20	0.07	-0.06	-0.04	0.08	0.03	0.02
r^{tot}_{μ}					0.36	0.34	0.26	0.33	0.23	-0.03	-0.05	-0.04	0.03	0.08	0.03
r^{tot}_{τ}						0.26	0.20	0.19	0.25	-0.03	-0.05	0.00	0.02	0.03	0.09
j^{tot}_{had}							0.79	0.70	0.64	-0.13	-0.24	-0.16	0.03	0.01	0.01
j^{tot}_{e}								0.58	0.53	-0.08	-0.20	-0.13	0.11	0.00	0.00
j^{tot}_{μ}									0.46	-0.09	-0.15	-0.12	0.02	-0.04	0.00
j^{tot}_{τ}										-0.08	-0.16	-0.08	0.02	0.00	-0.04
r^{fb}_{e}											0.04	0.03	0.09	0.00	0.00
r^{fb}_{μ}												0.05	-0.01	0.19	0.00
r^{fb}_{τ}													-0.01	0.00	0.18
j^{fb}_{e}														0.00	0.00
j^{fb}_{μ}															0.00

Table 2: Correlation matrix for the 16-parameters fit at LEP1 data.

	Γ_Z	r^{tot}_{had}	r^{tot}_{e}	r^{tot}_{μ}	r^{tot}_{τ}	j^{tot}_{had}	j^{tot}_{e}	j^{tot}_{μ}	j^{tot}_{τ}	r^{fb}_{e}	r^{fb}_{μ}	r^{fb}_{τ}	j^{fb}_{e}	j^{fb}_{μ}	j^{fb}_{τ}
M_Z	0.00	0.03	-0.01	0.02	0.01	-0.62	-0.38	-0.18	-0.16	0.04	0.08	0.06	0.00	-0.07	-0.06
Γ_Z		0.87	0.44	0.61	0.42	0.06	-0.01	0.03	0.03	0.01	0.02	0.02	0.03	0.05	0.05
r^{tot}_{had}			0.45	0.62	0.43	0.04	-0.02	0.02	0.02	0.01	0.02	0.02	0.03	0.05	0.04
r^{tot}_{e}				0.32	0.22	0.03	0.04	0.01	0.01	0.11	0.01	0.01	0.07	0.03	0.02
r^{tot}_{μ}					0.30	0.02	-0.02	0.09	0.01	0.01	0.03	0.02	0.02	0.11	0.03
r^{tot}_{τ}						0.02	-0.01	0.01	0.09	0.01	0.01	0.04	0.01	0.03	0.12
j^{tot}_{had}							0.27	0.15	0.14	-0.03	-0.06	-0.04	0.00	0.06	0.05
j^{tot}_{e}								0.08	0.07	0.02	-0.03	-0.02	0.13	0.03	0.03
j^{tot}_{μ}									0.04	-0.01	0.07	-0.01	0.00	0.34	0.02
j^{tot}_{τ}										-0.01	-0.01	0.08	0.00	0.02	0.34
r^{fb}_{e}											0.01	0.01	0.09	0.00	0.00
r^{fb}_{μ}												0.02	0.00	0.12	0.00
r^{fb}_{τ}													0.00	0.00	0.11
j^{fb}_{e}														0.00	0.00
j^{fb}_{μ}															0.01

Table 3: Correlation matrix for the 16-parameters fit at LEP1+LEP2 data.

	Γ_Z	r_{had}^{tot}	r_ℓ^{tot}	j_{had}^{tot}	j_ℓ^{tot}	r_ℓ^{fb}	j_ℓ^{fb}
M_Z	-0.42	-0.39	-0.32	-0.95	-0.82	0.26	0.04
Γ_Z		0.90	0.74	0.45	0.38	-0.09	0.05
r_{had}^{tot}			0.75	0.43	0.35	-0.08	0.05
r_ℓ^{tot}				0.35	0.33	-0.04	0.09
j_{had}^{tot}					0.81	-0.26	-0.03
j_ℓ^{tot}						-0.20	-0.04
r_ℓ^{fb}							0.17

Table 4: Correlation matrix for the 8-parameter fit at LEP1 data.

	Γ_Z	r_{had}^{tot}	r_ℓ^{tot}	j_{had}^{tot}	j_ℓ^{tot}	r_ℓ^{fb}	j_ℓ^{fb}
M_Z	0.00	0.03	0.01	-0.60	-0.33	0.10	-0.11
Γ_Z		0.87	0.70	0.06	0.03	0.03	0.07
r_{had}^{tot}			0.71	0.05	0.02	0.03	0.07
r_ℓ^{tot}				0.03	0.08	0.05	0.12
j_{had}^{tot}					0.26	-0.07	0.09
j_ℓ^{tot}						0.04	0.34
r_ℓ^{fb}							0.10

Table 5: Correlation matrix for the 8-parameter fit at LEP1+LEP2 data.

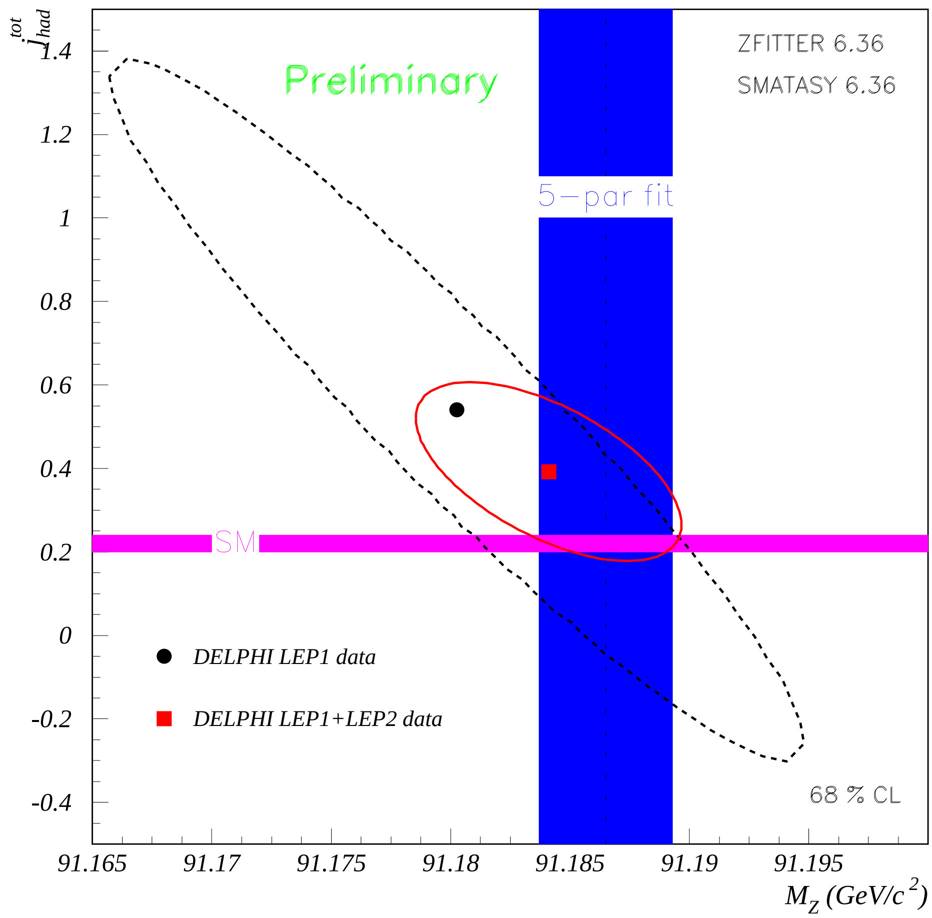

Figure 1: Contour plot in the M_Z-$j_{\rm had}^{\rm tot}$ plane. The dotted curve shows the region accepted at the 68% confidence level from a fit to data taken at the energies around Z^0; the solid curve shows the region accepted at the same confidence level when the high energy data are also included in the fit.

References

[1] P. Abreu *et al.*, Nucl. Phys. **B417** (1994) 3;
P. Abreu *et al.*, Nucl. Phys. **B418** (1994) 403;
P. Abreu *et al.*, E. Phys. J. **C16** (2000) 371.

[2] P. Abreu *et al.*, E. Phys. J. **C11** (1999) 383.

[3] P. Abreu *et al.*, Phys. Lett. **B485** (2000) 45.

[4] P. Abreu *et al.*, contributed paper to ICHEP (Osaka, July 2000), DELPHI 2000-128 CONF 427.

[5] A. Behrmann *et al.*, contributed paper to EPS HEP 2001 (Budapest, July 2001) and LP01 (Rome, July 2001), DELPHI 2001-094 CONF 522.

[6] D. Bardin *et al.*, Z. Phys. **C44** (1989) 493;
D. Bardin *et al.*, Comput. Phys.Comm. **59** (1990) 303;
D. Bardin *et al.*, Nucl. Phys. **B351** (1991) 1;
D. Bardin *et al.*, Phys. Lett. **B255** (1991) 290;
D. Bardin *et al.*, **CERN-TH 6443/92** (May 1992);
D. Bardin *et al.*, Comput. Phys. Commun. **133** (2001) 229.

[7] R. G. Stuart, Phys Lett. **B272** (1991) 353;
A. Leike, T. Riemann and J. Rose, Phys Lett. **B273** (1991) 513;
T. Riemann, Phys Lett. **B293** (1992) 451.

[8] S. Kirsch, T. Riemann, Comput. Phys. Commun. **88** (1995) 89.